Shifted-contour auxiliary-field Monte Carlo for molecular electronic structure

Naomi Rom, Eyal Fattal, Ashish K. Gupta, Emily A. Carter, and Daniel Neuhauser[a)]
Department of Chemistry and Biochemistry, University of California, Los Angeles, California 90095-1569

(Received 4 June 1998; accepted 12 August 1998)

The shifted-contour auxiliary-field Monte Carlo (SCAFMC) approach has been recently developed by Rom, Charutz and Neuhauser as an extension of the auxiliary-field Monte Carlo (AFMC) method. AFMC replaces the difficult fully interacting electrons problem by an ensemble of simpler problems where the electrons interact with a fluctuating electric field but not with each other. SCAFMC is based on shifting the auxiliary-field contour of integration to pass through the (imaginary) stationary point, leading to numerical stability at long propagation times. The new approach converges to the full CI energy in electronic structure calculations (both ground and low-lying excited states). Here we expand the application of SCAFMC from atomic to molecular problems. First, we calculate ground-state energies of a highly correlated transition-metal system (Cr_2) with a moderate (12 orbitals) active space size, and demonstrate that SCAFMC is able to extract the energies accurately. In addition, we use SCAFMC to calculate a C–C bond-stretch energy in ethane with complete active spaces of up to 28 orbitals. © *1998 American Institute of Physics.* [S0021-9606(98)30543-7]

I. INTRODUCTION

Recently, a potentially very powerful approach was introduced to electronic structure calculations,[1–3] the auxiliary-field Monte Carlo (AFMC) method, based on the Hubbard-Stratonovich transformation.[4,5] The method avoids the difficult calculation of a multielectron wave function and its properties. Instead, an ensemble of much simpler independent-particle problems is solved. The appealing feature of AFMC is that for a given single-particle orbital basis (or grid representation) it converges to the full CI (FCI) values associated with that basis, potentially without the factorial increase in computation time. AFMC has established itself as a powerful tool for many physical applications,[6–9] including, e.g., Hubbard model,[10–12] nuclear models[13,14] and homogeneous Jellium model[1,15] calculations.

AFMC was first applied to electronic structure calculations by Sorella, Baroni, Car and Parrinello who used a grid AFMC approach to calculate potentials for H_2,[9] and later by Charutz and Neuhauser[2] who evaluated ground state energies of He and Be. Convergence was quite poor, however, due to large oscillations[16] of a complex integrand (see Sec. II), which made AFMC inapplicable to larger atoms and molecules.

To alleviate these problems we recently introduced a modification named Shifted-Contour Auxiliary-Field Monte Carlo (SCAFMC),[3] which differs from AFMC in the Hamiltonian division of one- and two-body operators. In SCAFMC the primary quantity is not the density operator ρ but the fluctuation operator: $\rho - n$, where n is a fixed reference density. By working with the fluctuation operator, the two-body interaction is modified to include only the exchange-correlation part whereas the one-body interaction increases by the appropriate direct electron-electron interaction contribution. The oscillations of the complex integrand in the Hubbard-Stratonovich transformation are dramatically reduced in SCAFMC compared with AFMC, and accurate, numerically stable results are obtained for much larger systems than with AFMC.

Our goal here is to demonstrate the applicability of SCAFMC for molecules. So far, SCAFMC was successfully applied to extract ground and low-lying excited states of Ne.[3] The effort in the method, per ensemble member, scales between A^3 (where A is the number of electrons) and N^4 (where N is the spatial molecular-orbital basis-set size) depending on whether a grid, pseudo-grid or basis-set representation is used. This scaling needs to be multiplied by the number of ensemble members. Thus if the method converges well without an exponentially rising number of ensemble members, then it can be used as a viable alternative to coupled-cluster or full-CI methods which scale at least as N^8 ($N!$ for full CI).

The paper is organized as follows. After reviewing AFMC and SCAFMC (Sec. II), we turn to two nontrivial large ground-state basis-set simulations, involving 12 spatial molecular orbitals for Cr_2 (Sec. III) and up to 28 spatial orbitals for C_2H_6 (Sec. IV), followed by conclusions. An appendix discusses several approaches for extracting ground and excited-state energies.

II. THEORY

A. The molecular Hamiltonian

The starting point is the basic electronic-structure pair-interaction Coulomb Hamiltonian in a second quantization formalism (the method is equally useful in a grid formulation):

[a)]Electronic mail: dxn@chem.ucla.edu

$$H=h_1+h_2\equiv K\cdot\rho+\frac{1}{2}\rho\cdot V\cdot\rho$$
$$\equiv\sum_{\alpha\beta=1}^{N}K_{\alpha\beta}\rho_{\alpha\beta}+\frac{1}{2}\sum_{\alpha\beta\gamma\delta=1}^{N}v_{\alpha\beta\gamma\delta}\rho_{\alpha\beta}\rho_{\gamma\delta}, \tag{1}$$

where α, β, γ, and δ denote spatial molecular orbital indices. Here $\rho_{\alpha\beta}$ is defined in terms of the creation and destruction operators as $\rho_{\alpha\beta}=a_\alpha^+ a_\beta(\text{spin up})+a_\alpha^+ a_\beta(\text{spin down})$, while v is the appropriate matrix element of the electron-electron repulsion. K includes the kinetic energy ($T_{\alpha\beta}$), electron-nuclear attraction ($V_{\alpha\beta}^{eN}$) and a self-interaction part of the electron-electron repulsion terms:

$$K_{\alpha\beta}=V_{\alpha\beta}^{eN}+T_{\alpha\beta}-\frac{1}{2}\sum_{\gamma}v_{\alpha\gamma\gamma\beta}.$$

In the applications below we freeze a set of core orbitals, i.e., follow a standard electronic-structure practice and carry out the computation only with a valence Hamiltonian, H_{val}, and determinants, Φ_{val}, which are defined by the requirement:

$$\langle\Phi_{\text{val}}|H_{\text{val}}|\Phi_{\text{val}}\rangle=\langle\Phi_{\text{core}}\Phi_{\text{val}}|H_{\text{tot}}|\Phi_{\text{core}}\Phi_{\text{val}}\rangle, \tag{2}$$

for any determinant of the form $|\Phi\rangle=|\Phi_{\text{core}}\Phi_{\text{val}}\rangle$. The AFMC or SCAFMC calculations are then carried out only for the valence orbitals (i.e., they are applied to H_{val} while the core orbitals are fixed). Alternately, an effective core can be used.

B. Spectral information from propagator: Basics

AFMC and SCAFMC calculate, as shown below, the action of the propagator on an initial wave function, $e^{-H\tau}\Phi_0$. The simplest way to extract the ground-state energy is from:

$$E_0=\lim_{\tau\ \text{large}}E_0(\tau), \tag{3}$$

where

$$E_0(\tau)=\frac{\mathscr{H}(\tau)}{\mathscr{S}(\tau)}, \tag{4}$$

and

$$\mathscr{H}(\tau)=\langle\Phi_0|He^{-H\tau}|\Phi_0\rangle, \tag{5}$$

$$\mathscr{S}(\tau)=\langle\Phi_0|e^{-H\tau}|\Phi_0\rangle, \tag{6}$$

or directly from the correlation function $\mathscr{S}(\tau)$, which fulfills

$$\mathscr{S}(\tau)=\sum_j|a_j|^2e^{-E_j\tau}=\lim_{\tau\ \text{large}}|a_0|^2e^{-E_0\tau}. \tag{7}$$

Here a_j is the weight of the jth eigenstate in Φ_0. (We also use filter-diagonalization for extracting the correlation energies, as detailed in the Appendix.)

C. AFMC

The most important step in the AFMC derivation is the Hubbard-Stratonovich (HS) transformation, which replaces the calculation of the full propagator with a simpler calculation of an ensemble average of *single*-particle propagators. In each propagator, the electron-electron repulsion is absent, and instead the electrons interact with a fluctuating (time- and space-dependent) field.

The basic HS identity is

$$e^{-(c/2)y^2}=\sqrt{\frac{c}{2\pi}}\int e^{-(c/2)\sigma^2}e^{-ic\sigma y}d\sigma, \tag{8}$$

where c is a positive number and y can be an operator. The crucial point of Eq. (8) is that even if y is an operator (essentially the density operator, see below) the ''auxiliary-field'' σ is still just a number here, so that the action of each ''one-body propagator'' $e^{-ic\sigma y}$ on an initial Slater determinant is simple to evaluate.

Equation (8) applies to the evaluation of the propagator by using a large number (L) of small time-steps (dt), with a Trotter separation to h_1 and h_2: $e^{-H\tau}\approx\Pi_i e^{-h_1dt_i}e^{-h_2dt_i}$. The HS transformation is then readily shown (using the spectral representation of v) to yield for the single time-step electron-electron repulsion part of the propagator:

$$e^{-h_2dt}=\text{const}\cdot\int e^{-(1/2)(\sigma,v\sigma)dt}e^{-i(\sigma,v\rho)dt}\Pi_{\alpha\beta}(d\sigma_{\alpha\beta}), \tag{9}$$

with $(\sigma,v\rho)\equiv\Sigma_{\alpha\beta\gamma\delta=1}^{N}\sigma_{\alpha\beta}v_{\alpha\beta\gamma\delta}\rho_{\gamma\delta}$, and $(\sigma,v\sigma)$ defined analogously. Collecting Eqs. (1) and (9) and noting that a separate field $\sigma_{\alpha\beta}(t_l)$ needs to be used at each time ($t_l=ldt$, $l=1,\ldots,L$, and $\tau=Ldt$), it follows that the propagator $e^{-H\tau}$ can be written as:

$$e^{-H\tau}=\frac{\int P(\sigma)U_\sigma(\tau)D\sigma}{\int P(\sigma)D\sigma}, \tag{10}$$

where the weight is

$$P(\sigma)=e^{-(1/2)((\sigma v\sigma))},$$

and

$$((\sigma v\sigma))\equiv dt\cdot\sum_l(\sigma(t_l),v\sigma(t_l)),$$

while the measure refers to the whole set of time-dependent external fields, σ:

$$D\sigma\equiv\Pi_{l,\alpha\beta}d\sigma_{\alpha\beta}(t_l).$$

Finally, U_σ is a time-dependent one-body propagator,

$$U_\sigma(t_l)=\exp(-h^\sigma(t_l)\cdot\rho dt)U_\sigma(t_{l-1}), \tag{11}$$

associated with the time-dependent one-body Hamiltonian

$$[h^\sigma(t_l)]_{\alpha\beta}=K_{\alpha\beta}+i\sum_{\gamma\delta}v_{\alpha\beta\gamma\delta}\sigma_{\gamma\delta}(t_l). \tag{12}$$

Substituting Eq. (10) into Eq. (4) gives

$$\mathscr{H}(\tau)=\frac{\int P(\sigma)\langle\Phi_0|H|\Phi_\sigma(\tau)\rangle D\sigma}{\int P(\sigma)D\sigma},$$

while

$$\mathscr{S}(\tau)=\frac{\int P(\sigma)\langle\Phi_0|\Phi_\sigma(\tau)\rangle D\sigma}{\int P(\sigma)D\sigma}, \tag{13}$$

where

$$|\Phi_\sigma(\tau)\rangle = U_\sigma|\Phi_0\rangle. \tag{14}$$

The multidimensional integrals over σ in Eq. (13) are evaluated using a Monte Carlo algorithm, with the positive weight $P(\sigma)$. Note that the exponent in the Gaussian weight $1/2((\sigma v \sigma))$ is exactly the time-integral of the self-energy of the random time-dependent field, σ. Thus one needs to randomly pick a density σ according to its self-energy.

The final equation for $\mathscr{S}(\tau)$ is then

$$\mathscr{S}(\tau) = 1/N_{\text{sample}} \sum_\sigma \langle\Phi_0|\Phi_\sigma(\tau)\rangle, \tag{15}$$

where N_{sample} is the number of Monte Carlo sampling used. $\mathscr{H}(\tau)$ is similarly defined.

The practical evaluation of the integrals is very simple. Since each time-dependent propagator $U_\sigma(t)$ is a one-body propagator, its action on a single-determinant $|\Phi_0\rangle$ is straightforward: a new determinant is produced, $|\Phi_\sigma(t)\rangle$. The orbitals in this determinant, denoted by $\phi_k^\sigma(\mathbf{x},t)$ (k is an index over the orbitals), are obtained by time-dependent propagation of the initial orbitals $\phi_k(\mathbf{x})$ in the determinant $|\Phi_0\rangle$ under the one-body Hamiltonian h^σ. Expanding the orbitals in terms of the fixed basis-set $\chi_\beta(\mathbf{x})$ used for constructing H and using $\zeta_{\beta k}^\sigma(t)$ to denote the expansion coefficients yields:

$$\zeta_{\beta k}^\sigma(t) = \sum_\alpha \exp(-h^\sigma(t_l)dt)_{\beta\alpha}\zeta_{\alpha k}^\sigma(t-dt). \tag{16}$$

The overlap of the determinants is related to the determinant of the individual orbital overlaps:

$$\langle\Phi_0|\Phi_\sigma(t)\rangle = \det(\langle\phi_k|\phi_{\sigma k'}\rangle))^2$$

(the 2 is due to the spin contribution). Finally, Eqs. (4) and (7) or filter-diagonalization (Appendix) are used to extract the ground-state energy. However, as mentioned previously,[2,3] even for the Be atom the monotonic relaxation of $E_0(\tau)$ to E_0 is spoiled by large oscillations of the complex integrand, $\langle\Phi_0|\Phi_\sigma(\tau)\rangle$.

D. Shifted contour AFMC

In order to overcome the numerical instability which characterizes and limits the potential use of AFMC in electronic structure applications, the contour of integration in the σ plane is modified to pass through a stationary point. Formally, i times the HF density furnishes approximately a stationary point.[7] To see this in physical terms, note that H can be rewritten as

$$H = \tilde{h}_1 + \tilde{h}_2 \equiv \sum_{\alpha\beta} (K_{\alpha\beta} + (W_0)_{\alpha\beta})\rho_{\alpha\beta} + \frac{1}{2}\sum_{\alpha\beta\gamma\delta} (\rho_{\alpha\beta} - n_{\alpha\beta}) v_{\alpha\beta\gamma\delta}(\rho_{\gamma\delta} - n_{\gamma\delta}) + \text{const}, \tag{17}$$

where

$$(W_0)_{\alpha\beta} = \sum_{\gamma\delta} v_{\alpha\beta\gamma\delta} n_{\gamma\delta}.$$

One intuitive, physical choice of $n_{\alpha\beta}$ is the ground state HF density. If the molecular orbitals used to construct $K_{\alpha\beta}$ and $v_{\alpha\beta\gamma\delta}$ are the HF orbitals, and a closed-shell system with A electrons is used, then n has a particularly simple form:[17]

$$n_{\alpha\beta} = 2\delta_{\alpha\beta}, \quad \alpha < A/2.$$

W_0 is the direct part of the mean-field interaction. Thus $\tilde{h}_1$ includes also the main, direct electron-electron part of the mean-field portion of the electron-electron repulsion (through n), while only Hartree-Fock exchange and correlation remain in $\tilde{h}_2$ (via $\rho - n$). (In principle, the Hartree-Fock exchange can also be incorporated in W_0.[7])

Applying the HS transformation to the newly divided Hamiltonian [Eq. (17)] produces an expression for $\mathscr{S}(\tau)$ [and a similar one for $\mathscr{H}(\tau)$] whereby (in the numerator) σ is shifted to $\sigma - in$, $h_\sigma(t_l) \to h_\sigma(t_l) + W_0 = h_{\sigma - i\eta}$, and therefore $U_\sigma(\tau) \to U_{\sigma - i\eta}(\tau)$:

$$\mathscr{S}(\tau) = \frac{\int P(\sigma - in)\langle\Phi_0|U_{\sigma - in}(\tau)|\Phi_0\rangle D\sigma}{\int P(\sigma) D\sigma}. \tag{18}$$

Hence modifying the H division is equivalent to shifting the auxiliary density σ to a line with a fixed imaginary part $-in$. The computational benefit of this change is that the integrand oscillations are greatly reduced. Qualitatively note that the oscillating part for a single time-step becomes

$$e^{-i\sigma V\rho dt} \to e^{-i\sigma V(\rho - n)dt}.$$

Since $\rho - n$ is heuristically ''smaller'' than ρ, the oscillating integrand is smaller leading to less oscillations. These oscillations are replaced by the addition of a damping factor to the integrand: $e^{-W_0\rho dt}$. As a result, the numerical noise is diminished up to much longer values of τ.

As in AFMC, the SCAFMC expression [Eq. (18)] is evaluated using the Monte Carlo algorithm. Specifically, note that the *same* positive weight, $P(\sigma)$, is used here. Thus in practical terms, one evaluates:

$$\mathscr{S}(\tau) = \sum_\sigma \frac{P(\sigma - in)}{P(\sigma)}\langle\Phi_0|\Phi_{\sigma - in}\rangle = e^{+(1/2)((nvn))}\sum_\sigma e^{i((nv\sigma))}\langle\Phi_0|\Phi_{\sigma - in}\rangle, \tag{19}$$

and $\mathscr{H}$ similarly defined.

III. AN APPLICATION TO A HIGHLY CORRELATED SYSTEM: THE CHROMIUM DIMER

We have chosen the chromium dimer example in order to demonstrate and emphasize that our method can cope with the following types of molecular systems:

(1) Highly correlated electronic systems. First row transition metals (TM's) in particular, and especially those in the middle of the transition series, pose extremely challenging problems for the treatment of electron correlation. First row TM dimers are among the most difficult to treat because of the low overlap between d-orbitals. Fur-

TABLE I. Valence double-ζ basis set for Chromium: Cartesian Gaussian functions with exponents (α_i) and contraction coefficients (C_i).

Type	α_i	C_i	Type	α_i	C_i
s	7323	0.020 137 37	*p*	310.7	0.031 104 17
s	1104	0.139 510 84	*p*	72.25	0.194 565 78
s	249.2	0.482 195 52	*p*	21.98	0.520 835 12
s	67.76	0.496 864 86	*p*	7.332	0.431 657 61
s	97.38	−0.120 707 44	*p*	4.869	0.056 859 16
s	15.22	0.459 942 71	*p*	2.173	0.533 143 13
s	5.839	0.628 264 78	*p*	0.6657	0.523 192 70
s	9.576	−0.220 452 99	*p*	1.754	−0.033 956 14
s	1.688	0.533 599 53	*p*	0.1071	1.004 463 36
s	0.6096	0.601 910 46			
			p	0.029 84	1.000 000 00
s	0.9098	−0.342 730 64			
s	0.083 58	1.091 850 77	*d*	28	0.034 962 44
			d	7.213	0.190 597 28
s	0.029 61	1.000 000 00	*d*	2.241	0.455 347 58
			d	0.6612	0.577 838 96
			d	0.162	1.000 000 00

ther, as one goes to the middle of the row, one increases the number of open shell electrons on the atom and this poses a combinatorially more difficult spin coupling optimization problem. Chromium is the most extreme case since its ground-state valence electronic configuration in the atom is s^1d^5, i.e., both the *s* and all the *d* electrons are open shell. Thus the chromium dimer serves as an excellent test case for a method's ability to treat electron correlation and is used by many researchers as a benchmark for their methods.[18]

(2) Systems with a high density of states (with near degeneracy) in the vicinity of the ground state. This is also typical for TM's, where many spin states are in very close vicinity energetically to the ground state. Only a very stable numerical approach can converge to the ground state, i.e., resolve it from all other close in energy states. Again, the chromium dimer serves as a good test case.

Many *ab initio* theoretical methods have been implemented to compute the potential energy surface of this molecule.[18] Results of such studies have led over the years to conflicting results which span from a prediction of a very shallow (0.35 eV) minimum[19] to a strongly bound molecule with short intermolecular distance and a high bond order.[20,21] The studies do not all agree even on the symmetry of the ground state. The source of these problems lies in the numerical difficulty given above.

Experimental data for Cr_2 is available. A variety of experimental methods were used to study the chromium dimer: negative-ion photoelectron spectroscopy of CR_2^- (Refs. 22 and 23) collision-induced dissociation of CR_2^+ by Xe using guided ion beam mass spectrometry,[24] fluorescence excitation spectra of CR_2 produced by pulsed YAG laser vaporization of chromium metal[25,26] and Knudsen cell mass spectrometry.[27] These measurements demonstrate that the chromium dimer has a very short bond[25] of $R_e = 1.68$ Å, a vibrational frequency[23] of $\omega_e = 480\ \mathrm{cm}^{-1}$, and a substantial bond dissociation energy[26,24] $D_e = 1.45$ eV, giving evidence of multiple bonding. The uncongested fluorescence spectrum[26] is consistent with a $^1\Sigma_g^+$ ground state. Further, there is experimental evidence that the potential surface has a ''shelflike'' feature (i.e., almost a double minimum).[23]

We have used an all-electron valence double zeta basis[28] for the calculation, shown in Table I. We first calculate a generalized valence bond perfect pairing (GVB-PP) wave function[29] and then use it as a guess and as the *N*-particle basis for the SCAFMC method. GVB-PP provides an inexpensive MCSCF starting point for multireference CI calculations and such GVB-MRCI calculations have shown ubiquitously in the past to yield excellent binding energies and electronic excitation energies (e.g., the so-called correlation-consistent configuration interaction method of Carter and Goddard).[30–40] Couty and Hall have recently demonstrated that the choice of orbitals for CAS-CI calculations (a full valence CI where the orbital shapes are not updated as in CASSCF) is crucial and that localized orbitals yield much lower CAS-CI total energies than when symmetry-adapted orbitals are used.[41] GVB not only describes the chemical bond qualitatively correctly but also provides the only variational localization method as a by-product, while some of the localization procedures based on a HF wave function may fail. We have also recently shown the superiority of using GVB-PP orbitals as an initial guess to CASSCF, with regard to quicker convergence and convergence to the lowest energy wave function.[42]

The SCAFMC method application herein is to show how SCAFMC can reproduce CAS-CI calculations, namely a full CI within a set of valence orbitals. The orbitals we use here are precisely the GVB-PP orbitals from a calculation involving six GVB pairs ($s-s$ plus five $d-d$ bonds) which leads to a total of 12 natural orbitals [a so-called GVB(6/12)-PP calculation]. Thus the configuration space for the SCAFMC calculation contained all configuration state functions formed from all possible occupations of 12 electrons in these 12 orbitals.

The results of the SCAFMC were compared to a tradi-

tional CAS-CI calculation giving the same numbers up to the accuracy of the calculation, i.e., $(2-3)\times 10^{-3}$ a.u. The traditional CAS-CI total energies calculated are -2084.366 a.u. for 2.0 Å, and -2084.407 a.u. for 9.8 Å. For SCAFMC CAS-CI total energies calculated are -2084.365 (± 0.002) a.u. for 2.0 Å, and -2084.405 (± 0.003) a.u. for 9.8 Å. The difference between the results is both due to the small Monte Carlo sampling error (we used 400 000 samples for $R=2$ Å and 480 000 for $R=9.8$ Å to bring the error to 0.002 and 0.003 a.u., respectively), and in addition due to the small systematic error caused by the finite size of the time step, $dt=0.1$ a.u. In future studies we would show the dependence on dt. (More sophisticated propagation techniques can reduce this dt dependence.)

As can be seen the CAS-CI energies obtained by both methods lead to the conclusion that Cr_2 is unbound. This is a well known problem which is typical for highly correlated TM dimers (such as Cr_2 and Fe_2), namely, in such highly correlated systems one should extend the correlation space by including excitations to higher lying unoccupied orbitals in order to obtain correct binding energetics. While SCAFMC can easily go beyond the CAS(12/12)-CI due to its $O(N^4)$ numerical scaling, traditional full CI cannot since it obeys factorial numerical scaling. In the future we intend to address the given problem of Cr_2, as opposed to merely a proof of method given here, by using SCAFMC to calculate Cr_2 using an extended correlation space (a full CI of 12 electrons in 18 or 24 orbitals).

To appreciate the intrinsic difficulty in the calculations, we note that the total valence energy was higher than 20 a.u. for $R=2$ and 9.8 Å, respectively. The correlation energy (i.e., the CI result with the HF subtracted) is large (0.965 a.u. and 2.042 a.u., respectively). Still, the accuracy was 0.002 to 0.003 a.u. The initial wave function in all calculations is, as mentioned, a closed-shell Slater determinant made from the lowest energy GVB-PP orbitals in each study. For $R=2$ Å this wave function has a reasonably large overlap with the true ground state, as determined by the long time-evolution of the correlation function, $\mathscr{S}(\tau)\rightarrow |a_0|^2 \exp(-E_0\tau)$ (see Fig. 1). For the asymptotic calculation (at 9.8 Å), the single closed-shell Slater-determinant of the dominant configuration in the GVB-PP orbitals is (as is well known) a very poor approximation to the ground state, so $|a_0|^2 \sim 0.002$. Even in this challenging case, the Auxiliary-Field Monte Carlo works very well, extracting accurately the ground-state energy (Fig. 2).

Figure 3 shows another aspect of AFMC, the individual contributions to the Monte-Carlo summation over $\mathscr{S}(\tau)$ [Eq. (19)]. The figure shows that while at short times even a small-sample average (over 100 time points) is well behaved, an individual contribution fluctuates widely and at times has a very small amplitude (10^5 times smaller than the average). This confirms that even with the Shifted-Contour contribution, AFMC is far from being a perturbation expansion with small perturbations.

IV. ETHANE C–C BOND ENERGY

In addition to the highly correlated transition metals, we have also checked SCAFMC on hydrocarbons, where the correlation energies are much smaller. Specifically, the carbon–carbon bond stretch energy in ethane was computed using SCAFMC, and the results were compared to GAUSSIAN 94 quadratic singles and doubles configuration interaction with perturbative triple excitations [QCISD(T)] calculations, using the same basis set, 6-31G, for the carbon and hydrogen atoms (the maximal size of the basis set is $N_{C_2H_6}=30$). The two lowest orbitals (carbon $1s$) were treated as a fixed core, leaving 14 (out of 18) electrons in the active orbitals. Three different basis sizes (active orbitals) were tested for: 15, 20 and 28. In Table II we present the SCAFMC results (first line) for the three different sets of basis parameters along with the appropriate CI values (second line), at two C–C distances: 1.54 Å (equilibrium geometry) and 3.54 Å. Both the C–H distance and H–C–H angle were kept fixed at 1.095 Å and 111.18° in all calculations, so that the energy

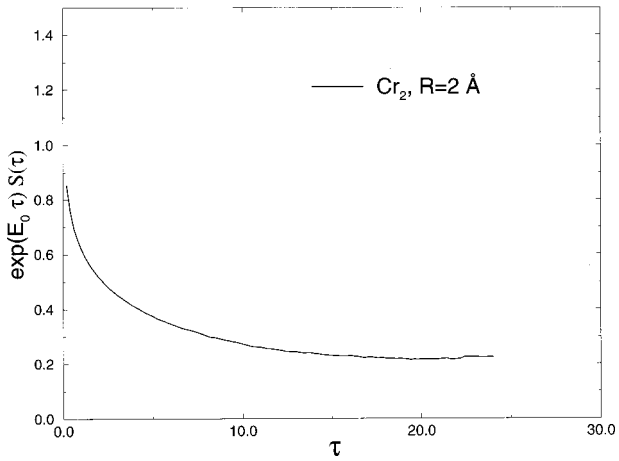

FIG. 1. The AFMC correlation function for Cr_2 at $R=2$ Å. The correlation function $S(\tau)$ was multiplied by $e^{E_0\tau}$ (where E_0 was determined by filter-diagonalization). Asymptotically, $e^{E_0\tau}S(\tau)$ should reach a constant. This run employed 400 000 Monte Carlo samples, with $dt=0.1$ a.u. The energy extracted from the run is -2084.365 ± 0.002 a.u., in accordance with full-CI calculations (-2084.366 a.u.).

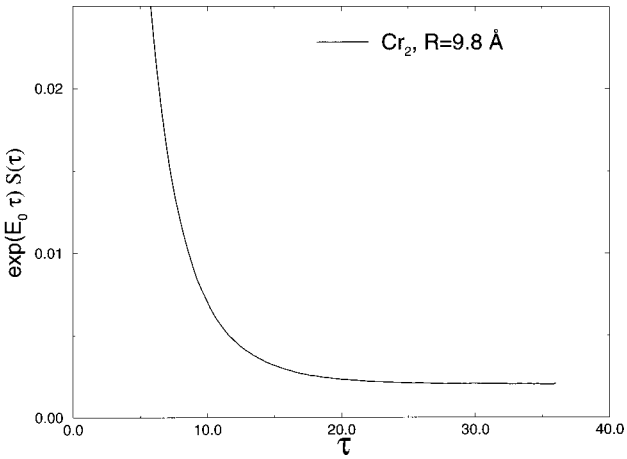

FIG. 2. The AFMC correlation function for Cr_2 at $R=9.8$ Å, using 480 000 Monte Carlo samples. The asymptotic value of $e^{E_0\tau}S(\tau)$ is very small (0.0022) since the initial wave function is a Hartree-Fock determinant of the closed-shell GVB-PP molecular orbitals, which, due to the large distance between the fragments, has very little overlap with the true ground state.

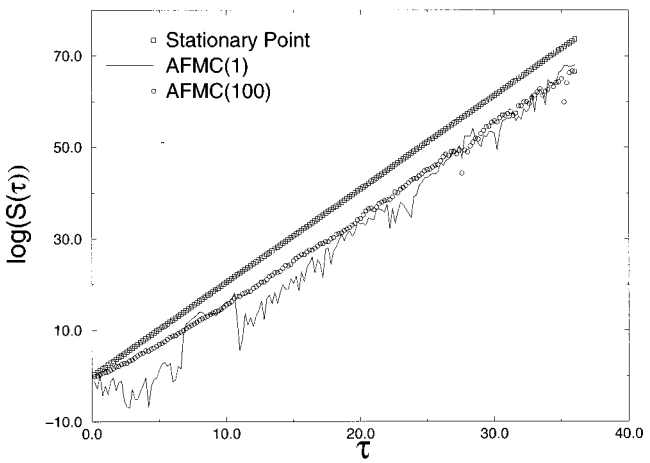

FIG. 3. Cr_2 at $R=9.8$ Å. The real part of the contribution $[P(\sigma-in)/P(\sigma)]\langle\Phi_0|\Phi_{\sigma-in}\rangle$ of a single trajectory to $S(\tau)$ and an average over 100 trajectories to obtain $S(\tau)$, plotted on a logarithmic scale. In addition, the same term is plotted for the approximate stationary point of the AFMC integrand on the imaginary axis at $\sigma=-in$. Note that the individual contribution is at times wildly different than the overall average.

difference between the calculations at different C–C values provides a bond-stretching energy. As evident from the numerical values, the agreement between the SCAFMC results and the CI ones is excellent.

V. CONCLUSIONS

The application to molecular systems of SCAFMC, the recently developed version of the AFMC, was demonstrated through the nontrivial Cr_2 molecule and ethane bond-energy applications. The basis set sizes which were studied (up to $N=28$) and the number of electrons (up to 28) included in the quantum mechanical simulations unveil the applicability and potential of SCAFMC. Due to the shifting of the auxiliary field, σ, to the complex plane, the oscillatory behavior that was inherent in the AFMC approach is diminished, and the relaxation to the exact correlation energy is achieved for larger systems. The advantage of SCAFMC is its general applicability to different types of electronic correlations in molecular systems, while its modest scaling enables the treatment of large active spaces and many electrons.

Although SCAFMC is already working well for nontrivial molecular problems, it can be further improved. Specifically, we have recently shown that the Shifted-Contour modification is also able to diminish the fluctuations in a grid problem, where the per-ensemble-member effort scales quasilinearly with the grid size, rather than N^4 as in the basis-set representation.[43] Further, we have also recently demonstrated[44] in a model H_2 study that the method is very accurate in real-time simulations (of $\langle\Phi_m|e^{-iHt}|\Phi_{m'}\rangle$, see also the Appendix) which are very useful for both molecular spectra and for extracting high lying excited-state energies. [The equations for time-dependent SCAFMC are entirely equivalent to Eq. (18), except for the replacement of several ''i'' factors in the one-body terms by $\sqrt{i}$.[2,44]] Finally, the numerical convergence of the method can be further enhanced by a Filinov-like transform,[45–49] whereby the contribution of each trajectory is weighted by a factor which accounts for the fluctuations in nearby trajectories. We have recently derived such an approach for the molecular structure problem.[49] Eventually, a semiclassical approach to the method may prove the most accurate.

In this article we concentrated on ground-state applications, which could also be described by other very accurate approaches, e.g., trajectory-based fixed-node quantum Monte Carlo.[50–53] Eventually, we predict that SCAFMC will be most useful in two directions. First, for excited state and spectra (from subspace diagonalization and real-time applications). Second, SCAFMC looks promising for a consistent solution of the problem[54] of coupling of a highly accurate treatment of a subset of orbitals with more approximate treatments of a larger set of orbitals. Specifically, the Hubbard-Stratonovich transformation transforms the full-CI subset to a set of simpler problems. These can be treated, within each ensemble, using, e.g., imaginary-time density-functional propagation, applied to the whole set of orbitals (both those for which a full-CI treatment is desired and those for which only a more approximate evaluation is required). This approach may be useful, e.g., to the problem of a chemical reaction within a larger condensed phase environment.

TABLE II. SCAFMC ethane C–C bond-stretch energy (first line) versus QCISD(T) results obtained from GAUSSIAN 94 (second line) for different CI basis-set sizes. $N_{\rm orb}$ is the number of active (valence) orbitals used in the calculations, E_{eq} and E_∞ are the electronic energies at 1.54 Å and 3.54 Å C–C distances correspondingly, and ΔE is the ''bond stretch'' energy in kcal/mole (see text). The HF energies at 1.54 and 3.54 Å are -79.193 and -78.934 a.u., respectively. A 6-31G basis was used for the carbon and hydrogen atoms ($N_{C_2H_6}=30$).

$N_{\rm orb}$	Method	$E_{R=1.54\ \text{Å}}$ (a.u.)	$E_{R=3.54\ \text{Å}}$ (a.u.)	$\Delta E\left(\frac{\text{kcal}}{\text{mol}}\right)$
15	SCAFMC	−79.245	−79.099	91.6
15	QCISD(T)	−79.245	−79.103	89.1
20	SCAFMC	−79.308	−79.156	94.7
20	QCISD(T)	−79.307	−79.159	92.9
28	SCAFMC	−79.414	−79.271	89.5
28	QCISD(T)	−79.417	−79.274	89.7

ACKNOWLEDGMENTS

We thank R. Baer for extensive discussions and comments on the manuscript, and S. E. Koonin, R. Kosloff, G. Reynolds and S. Schwartz for helpful discussions. We also thank D. Charutz who contributed to developing the AFMC code. This work was supported by the NSF Early Career Award CHE-9502106, NSF fund CHE97-27084, the Alfred P. Sloan Fellowship (D.N.) and by NSF fund CHE95-27882 (E.A.C).

APPENDIX: EXTRACTING SPECTRAL INFORMATION FROM THE PROPAGATOR: DETAILS

There are several ways to extract ground and excited state energies from the propagator. One approach extends $E_0=\lim_{\tau\to\infty}\mathscr{H}(\tau)/\mathscr{S}(\tau)$, i.e., uses subspace diagonalization. Specifically, several (''M'') initial determinants, la-

beled as Φ_m, are chosen, and the action of $e^{-H\tau}$ is calculated on each. Then one solves the $M\times M$ matrix equation:

$$\mathscr{H}\mathbf{B}=\mathscr{S}\mathbf{B}\mathbf{E}, \tag{A1}$$

where $\mathscr{H}$, $\mathscr{S}$ are now $M\times M$ matrices with elements:

$$\mathscr{S}_{\mathbf{m},\mathbf{m}'}(\tau)=\langle\Phi_m|e^{-H\tau}|\Phi_{m'}\rangle,$$
$$\mathscr{H}_{\mathbf{m},\mathbf{m}'}(\tau)=\langle\Phi_m|He^{-H\tau}|\Phi_{m'}\rangle, \tag{A2}$$

evaluated as

$$\mathscr{S}_{m,m'}=1/N_{\text{sample}}\sum_{\sigma}\ \frac{P(\sigma-in)}{P(\sigma)}\langle\Phi_m|\Phi_{\sigma,m'}\rangle, \tag{A3}$$

$$\mathscr{H}_{m,m'}=1/N_{\text{sample}}\sum_{\sigma}\ \frac{P(\sigma-in)}{P(\sigma)}\langle\Phi_m|H|\Phi_{\sigma,m'}\rangle. \tag{A4}$$

An advantage of a multiple initial-determinant (i.e., $M>1$) calculation is that it speeds up the convergence in τ, and supplies low-lying excited states, from the eigenvalues of Eq. (A1).[3,55]

An alternative to Eq. (A1) is to evaluate the ground and excited state energies directly from $\mathscr{S}$, in analogy to Eq. (A3). Specifically, it is easy to show that the eigenvalues of $\mathscr{S}$, labeled by λ_j, are the exponentiated energies:

$$\mathscr{S}\mathbf{B}=\mathbf{B}\lambda, \tag{A5}$$

with

$$\lambda_j=\lim_{\tau\ \text{large}}\ e^{-E_j\tau}. \tag{A6}$$

Interestingly, the overlaps in Eq. (A3) can be evaluated very efficiently using the Sherman-Morrison technique.[2,56] When extracting eigenvalues directly from the $\mathscr{S}$ matrix [Eq. (A6)], the additional effort in calculating the matrix overlap scales then slowly, as $A^2N+A^2M^2$.

Finally, the eigenvalues can be extracted from $\mathscr{S}$ using filter-diagonalization (FDG).[57–60] FDG is a general approach to extract frequencies from correlation functions, based on the use of an energy-selected basis associated with the correlation functions. It can be used both for imaginary-time and real-time propagation. Here we quote only the final formulas (see, e.g., Ref. 60): one picks a set of N_E energies, $\{E\}$, in the desired energy range and diagonalizes the following $(N_E\cdot M)\times(N_E\cdot M)$ matrix equation:

$$\mathscr{G}C=\mathscr{F}Cu, \tag{A7}$$

where

$$\mathscr{G}_{Em,E'm'}=\int_0^{T/2}\int_0^{T/2}e^{iEt+E't'}\mathscr{S}_{m,m'}(t+t'+dt)dtdt',$$

and

$$\mathscr{F}_{Em,E'm'}=\int_0^{T/2}\int_0^{T/2}e^{iEt+E't'}\mathscr{S}_{m,m'}(t+t')dtdt'.$$

Here u is a diagonal matrix associated with the frequencies; for imaginary-time propagation it is

$$u_j=\exp(-E_jdt),$$

while for real-time propagation it is

$$u_j=\exp(-iE_jdt).$$

(Filter-diagonalization for SCAFMC can be applied of course to mixed real and imaginary propagation, of the form $e^{(-it+\tau)H}$.)

In our simulations, filter-diagonalization was the most accurate approach for extracting eigenvalues. The method intrinsically averages information over many time steps, thereby increasing its accuracy.

[1] P. L. Silvestrelli, S. Baroni, and R. Car, Phys. Rev. Lett. **71**, 1148 (1993).
[2] D. M. Charutz and D. Neuhauser, J. Chem. Phys. **102**, 4495 (1994).
[3] N. Rom, D. M. Charutz, and D. Neuhauser, Chem. Phys. Lett. **270**, 382 (1997).
[4] R. L. Stratonovich, Sov. Phys. Dokl. **2**, 416 (1958).
[5] J. Hubbard, Phys. Rev. Lett. **3**, 77 (1959).
[6] S. Levit, Phys. Rev. C **21**, 1594 (1980).
[7] J. W. Negele, Rev. Mod. Phys. **54**, 913 (1982).
[8] G. Sugiyama and S. E. Koonin, Ann. Phys. **168**, 1 (1986).
[9] S. Sorella, S. Baroni, R. Car and M. Parrinello, Europhys. Lett. **8**, 663 (1989).
[10] S. R. White, D. J. Scalapino, R. L. Sugar, E. Y. Loj, Jr., J. E. Gubernatis, and R. T. Scalettar, Phys. Rev. B **40**, 506 (1989).
[11] J. E. Hirsch, Phys. Rev. B **28**, 4059 (1983).
[12] S. Zhang, J. Carlson and J. E. Gubernatis, Phys. Rev. Lett. **74**, 3652 (1995).
[13] Y. Alhassid, D. J. Dean, S. E. Koonin, G. Lang, and W. E. Ormand, Phys. Rev. Lett. **72**, 613 (1994).
[14] M. Honma, T. Mizusaki, and T. Otsuka, Phys. Rev. Lett. **75**, 1284 (1995).
[15] M. T. Wilson and B. L. Gyorff, J. Phys.: Condens. Matter **7**, 371 (1995).
[16] D. R. Hamann and S. B. Fahy, Phys. Rev. Lett. **65**, 3437 (1990).
[17] This choice is used in the C_2H_6 simulations below. In the Cr_2 simulations we use the GVB-PP density-matrix, which, especially for extended-bond length, is much closer to the true density and is therefore a better shift. See also Baer, Head-Gordon, and Neuhauser (to be submitted).
[18] B. O. Roos, K. Andersson, M. P. Fulscher, P.-Å. Malmqvist and L. Serrano-Andres, Adv. Chem. Phys. **XCIII**, 219 (1996).
[19] M. M. Goodgame and W. A. Goddard III, Phys. Rev. Lett. **48**, 135 (1982).
[20] K. Andersson, B. O. Roos, P.-Å. Malmqvist, and P.-O. Widmark, Chem. Phys. Lett. **230**, 391 (1994).
[21] K. Andersson, Theor. Chim. Acta **91**, 31 (1995).
[22] S. M. Casey, P. W. Villalta, A. A. Bengali, C. L. Cheng, J. P. Dick, P. T. Fenn, and D. G. Leopold, J. Am. Chem. Soc. **113**, 6688 (1991).
[23] S. M. Casey and D. G. Leopold, J. Phys. Chem. **97**, 816 (1993).
[24] C.-X. Su, D. A. Hales, and P. B. Armentrout, Chem. Phys. Lett. **201**, 199 (1993).
[25] V. E. Bondybey and J. H. English, Chem. Phys. Lett. **94**, 443 (1983).
[26] V. E. Bondybey, Science **227**, 125 (1985).
[27] A. Kant and B. Strauss, J. Chem. Phys. **45**, 3161 (1966).
[28] This basis set was optimized for the D^n configuration of the metal as discussed in: A. K Rappe, T. A. Smedley, and W. A. Goddard III, J. Phys. Chem. **85**, 2607 (1981).
[29] F. W. Bobrowicz and W. A. Goddard III, ''The self-consistent field equations for generalized valence bond and open-shell Hartree-Fock wave functions'', in *Modern Theoretical Chemistry: Methods of Electronic Structure Theory*, edited by H. F. Schaefer III (Plenum, New York, 1977).
[30] E. A. Carter and W. A. Goddard III, J. Phys. Chem. **88**, 1485 (1984).
[31] E. A. Carter and W. A. Goddard III, J. Chem. Phys. **86**, 862 (1987).
[32] E. A. Carter and W. A. Goddard III, J. Phys. Chem. **91**, 4651 (1987).
[33] E. A. Carter and W. A. Goddard III, J. Chem. Phys. **88**, 1752 (1988).
[34] E. A. Carter and W. A. Goddard III, J. Chem. Phys. **88**, 3132 (1988).
[35] E. A. Carter and W. A. Goddard III, J. Phys. Chem. **92**, 2109 (1988).
[36] E. A. Carter and W. A. Goddard III, J. Am. Chem. Soc. **110**, 4077 (1988).
[37] C. J. Wu and E. A. Carter, J. Am. Chem. Soc. **112**, 5893 (1990).
[38] C. J. Wu and E. A. Carter, J. Phys. Chem. **95**, 8352 (1991).
[39] S. Khodabandeh and E. A. Carter, J. Phys. Chem. **97**, 4360 (1993).
[40] G. G. Reynolds and E. A. Carter, J. Phys. Chem. **98**, 8144 (1994).
[41] M. Couty and M. B. Hall, J. Phys. Chem. A **101**, 6936 (1997).
[42] E. Fattal, R. L. Hayes, and E. A. Carter (unpublished results).
[43] R. Baer, M. Head-Gordon, and D. Neuhauser, J. Chem. Phys. (in press).
[44] R. Baer and D. Neuhauser (in preparation).
[45] A. P. Vinogradov and V. S. Filinov, Sov. Phys. Dokl. **26**, 1044 (1981).

[46] R. D. Coalson, D. L. Freeman, and J. D. Doll, J. Chem. Phys. **7**, 4242 (1989).
[47] N. Makri and W. H. Miller, Chem. Phys. Lett. **139**, 10 (1987).
[48] C. H. Mak and D. Chandler, Adv. Chem. Phys. **93**, 39 (1996).
[49] D. Neuhauser (in preparation).
[50] A. B. Luchow and J. B. Anderson, J. Chem. Phys. **105**, 4636 (1996).
[51] P. J. Reynolds, B. J. Alder, D. M. Ceperley, and W. A. Lester, J. Chem. Phys. **77**, 5593 (1982).
[52] J. C. Grossman, L. Mitas, and K. Raghavachari, Phys. Rev. Lett. **75**, 3870 (1995).
[53] W. A. Lester, Annu. Rev. Phys. Chem. **41**, 283 (1990).
[54] N. Govind, Y. A. Wang, A. J. R. da Silva, and E. A. Carter, Chem. Phys. Lett. **295**, 129 (1998).
[55] D. M. Ceperley and B. Bernu, J. Chem. Phys. **89**, 6316 (1988).
[56] W. H. Press, S. A. Teukolsky, W. T. Vetterling, and P. P. Flannery, *Numerical Recipes* (Cambridge University Press, New York, 1992).
[57] M. R. Wall and D. Neuhauser, J. Chem. Phys. **102**, 8011 (1995).
[58] J. W. Pang, T. Dieckmann, J. Feigon, and D. Neuhauser, J. Chem. Phys. **108**, 8360 (1998).
[59] V. A. Mandelshtam and H. S. Taylor, Phys. Rev. Lett. **78**, 3274 (1997).
[60] E. Narevicius, D. Neuhauser, H. J. Korsch, and N. Moiseyev, Chem. Phys. Lett. **276**, 250 (1997).